Available online at www.sciencedirect.com

ScienceDirect

Journal of Magnesium and Alloys 1 (2013) 267–274
www.elsevier.com/journals/journal-of-magnesium-and-alloys/2213-9567

Full length article

Influence of incorporating Si_3N_4 particles into the oxide layer produced by plasma electrolytic oxidation on AM50 Mg alloy on coating morphology and corrosion properties

Xiaopeng Lu*, Carsten Blawert, Nico Scharnagl, Karl Ulrich Kainer

Helmholtz-Zentrum Geesthacht Zentrum für Material-und Küstenforschung GmbH, Institute of Materials Research, Max-Plank-Str. 1, 21502 Geesthacht, Germany

Abstract

The influence of incorporating different sizes of Si_3N_4 particles on the microstructure and corrosion properties of a phosphate-based plasma electrolytic oxidation (PEO) coating on AM50 magnesium alloy was investigated. The experiments for this study were performed in alkaline electrolytes containing 1 g/L KOH, 10 g/L Na_3PO_4 with and without three different sized of Si_3N_4 particles. The corrosion properties of PEO coatings were investigated by potentiodynamic polarization and electrochemical impedance spectroscopy (EIS) in 0.5 wt.% NaCl solution. Microstructure observations by SEM showed that the surface morphology and composition of the PEO coating were affected greatly by particle addition. Si_3N_4 particles can still be found without decomposition in the final coating due to their high melting point.

Keywords: Magnesium; Plasma electrolytic oxidation; Microstructure; Corrosion resistance

1. Introduction

Plasma electrolytic oxidation (PEO) is a promising process which produces relatively thick, ceramic-like coatings containing amorphous and crystalline phases, with incorporation of species originating from substrate and electrolyte [1–3]. This method is based on the anodic polarization of a metal in an aqueous electrolyte at high voltage that causes the occurrence of plasma micro discharges at the metal surface which converts the surface into a ceramic top coating. Unfortunately, the discharges create not only the coating, but also some defects, for example discharge channels, pores from gas inclusions and cracks. This has negative effects on the corrosion resistance. In order to improve the corrosion properties of PEO coated magnesium and its alloys, different particles suspended in the electrolyte have been incorporated into the coating to improve the microstructure. Examples of such particles include silica, titanium dioxide, alumina and zirconia [4–9].

Silicon nitride (Si_3N_4) has been frequently used and studied for its unique properties such as high hardness, high wear resistance, good inert chemical behavior and high temperature properties [10]. However, only little work has been done on the influence of corrosion resistance by incorporating Si_3N_4 particles into PEO coating for magnesium alloys. In this paper, three different sizes of Si_3N_4 particles have been incorporated into a plasma electrolytic oxidation coating from an alkaline electrolyte. The effect of different sizes of Si_3N_4 particles on the alteration of microstructural morphology and corrosion resistance are evaluated by different characterization methods.

* Corresponding author. Tel.: +49 4152871943; fax: +49 4152871960.
E-mail addresses: xiaopeng.lu@hzg.de (X. Lu), carsten.blawert@hzg.de (C. Blawert), nico.scharnagl@hzg.de (N. Scharnagl), karl.kainer@hzg.de (K.U. Kainer).
Peer review under responsibility of National Engineering Research Center for Magnesium Alloys of China, Chongqing University

Production and hosting by Elsevier

http://dx.doi.org/10.1016/j.jma.2013.11.001.

2. Experimental

An AM50 magnesium alloy with a nominal composition of (mass fraction) 4.7% Al, 0.38% Mn, max. 0.1% Zn, max. 0.1% Si, max. 0.002% Fe, max. 0.002% Cu, max. 0.001% Ni and Mg balance was used in this investigation. Specimens of size 15 mm × 15 mm × 4 mm were polished using 320, 500 and 1200 grit emery sheets successively and cleaned with ethanol before the PEO treatment. The PEO treatment was carried out using an unipolar pulsed power source with a pulse ratio of t_{on}:t_{off} = 2 ms:18 ms in electrolyte composed by 1 g of KOH and 10 g of Na_3PO_4 in 1 l of deionized water with additional 5 g of three different sizes of Si_3N_4 particles. The sizes of the three different Si_3N_4 particles varied from nano-particle to micro-sized particle, i.e. about 0.02 μm, 0.1–0.8 μm and 1–5 μm, which can be seen in Fig. 1. The smallest particles are agglomerated and the real shape is hardly to be seen but most likely globular. Medium-sized particles contain many fibers and globular particles. In the case of the largest particles, irregular and flaky particles can be observed. The same composition and concentration of alkaline electrolyte without particle was used for comparison and evaluation of the particle influence. During the PEO process, the magnesium alloy sample and stainless steel tube were used as the anode and cathode, respectively. All of the PEO treatments were performed at a constant voltage of 450 V for 10 min. The temperature of the PEO electrolytes was kept at 10 ± 2 °C by a water cooling system.

Scanning electron microscope (Cambridge Stereoscan) was used to examine the surface morphology and cross section of the PEO coatings. A Zeiss Ultra55 SEM equipped with an energy dispersive spectrometer (EDS) was used to determine the elemental composition and distribution of the PEO coatings. The phase composition analysis was done in a Bruker X-ray diffractometer equipped with Cu Kα radiation.

The corrosion behavior of the PEO coated magnesium alloy specimen was assessed by potentiodynamic polarization and electrochemical impedance spectroscopy (EIS) tests, which were carried out using an ACM Gill AC computer, controlled potentiostat. A typical three-electrode cell with the coated specimen as the working electrode (0.5 cm^2 exposed area), a saturated Ag/AgCl electrode as the reference electrode, and a platinum mesh as counter electrode was used. Polarization studies were carried out starting at −150 mV with reference to OCP (after 30 min of exposure at OCP) at a sweep rate of 0.2 mV s^{-1} until reaching a final current density of 0.01 mA cm^{-2}. Electrochemical impedance spectroscopy (EIS) studies were performed at open circuit potential with AC amplitude of 10 mV over the frequency range from 30 kHz to 0.01 Hz. The measurements were repeated at certain fixed times (0, 1, 3, 6, 12, and 24 h) up to 3 days of immersion time.

3. Results

3.1. Evolution of PEO coating

As a constant voltage of 450 V was used for performing the coating process in all the cases, the current decreased rapidly with the passage of time. For the PEO coating obtained from the electrolyte without particle addition, very fine sized discharges began to appear at a voltage termed as

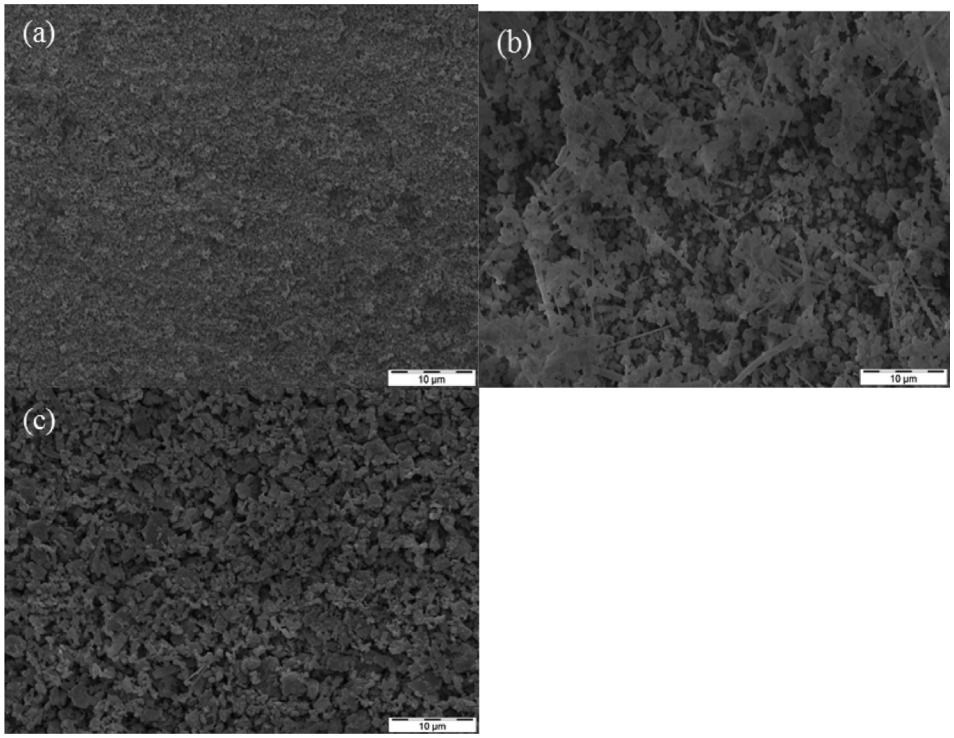

Fig. 1. SEM image of Si_3N_4 particles (a) 0.02 μm, (b) 0.1–0.8 μm, (c) 1–5 μm.

breakdown potential (250 V in this electrolyte). By increasing processing time, the size of the sparks grew and changed their color, in addition to the decrease of discharge density on the surface. The size, density and color variation of the sparks may be ascribed to the changes of the number and type of the active plasma species, the growth of the films and the applied energy [11]. The physical changes that might occur on the surface of PEO coating in electrolytes with particle addition cannot be observed due to the milky character of the solution. The only change one can see was the continuous decrease to 0.01 A of current accompanying with the constant voltage which is similar to PPEO. However, treatment was not successful in the case of using the 0.02 μm sized nanoparticles. The voltage could only reach 380 V and current remain at a high value (1.6 A). Therefore, PEO coating obtained from the electrolyte containing the 0.02 μm sized nanoparticles is excluded from further characterization of microstructure and properties. For ease of referencing, the coatings obtained in phosphate based electrolyte with smallest size (0.02 μm), medium size (0.1–0.8 μm), large-sized particle (1–5 μm) and without particle are named PPEO(S), PPEO(M), PPEO(L) and PPEO, respectively.

3.2. Microstructure

The surface morphologies of PPEO coated specimens are shown in Fig. 2. The typical morphology of PPEO coating presented in Fig. 2a reveals many micropores and some cracks on the surface. The size of those pores is in the range of 1–20 μm. These open pores are formed by the discharges and gas inclusions during PEO processing. Melted material has been expelled by the discharges and has solidified quickly before it could flow back to close the discharge channels. Significant change (Fig. 2c and e) can be observed on the surface of PEO coatings obtained in electrolytes with particle addition. On the one hand, many particles are sticking on the surface, indicating they might take part in PEO processing; on

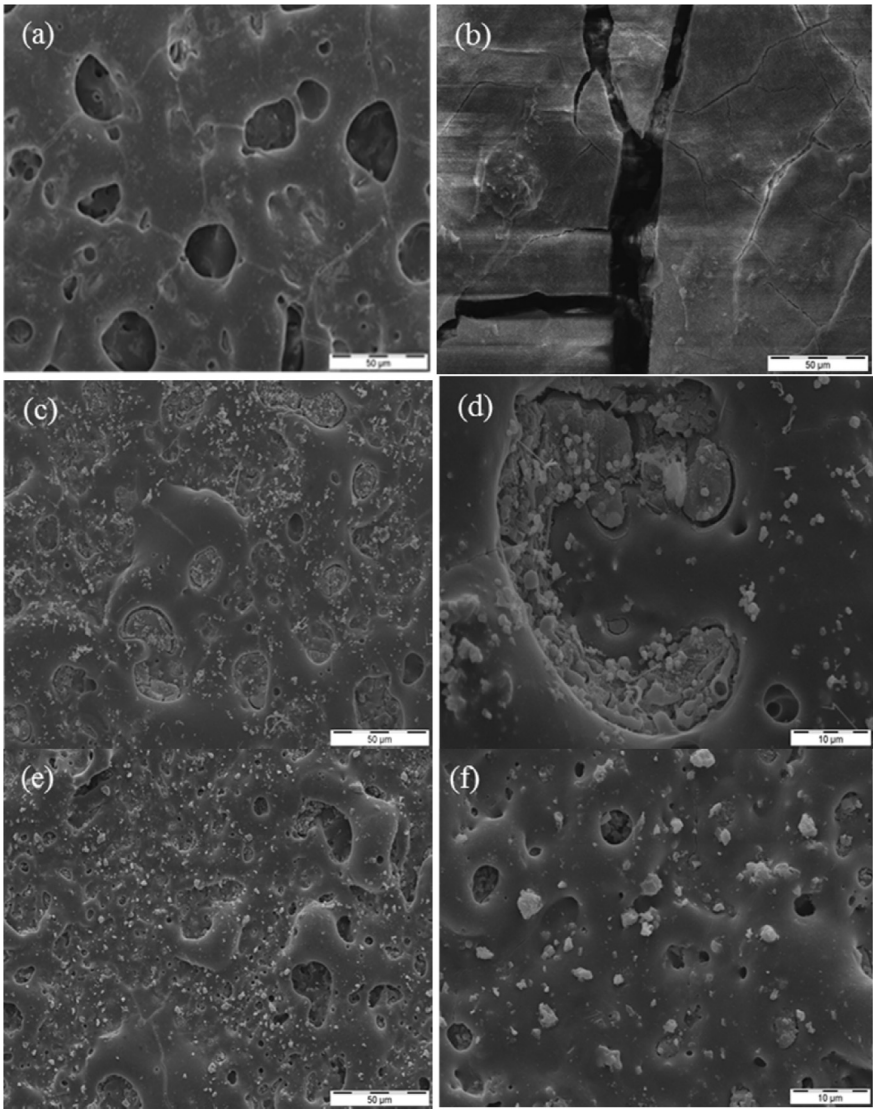

Fig. 2. Surface morphology of PPEO coatings (a) PPEO, (b) PPEO(S), (c) and (d) PPEO(M), (e) and (f) PPEO(L).

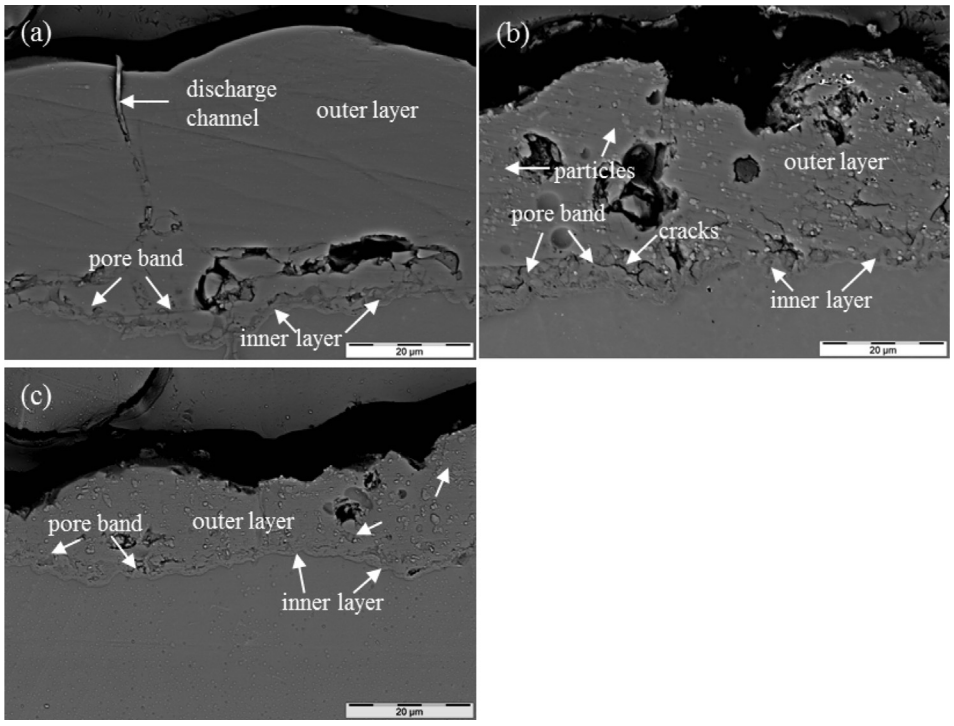

Fig. 3. Backscattered scanning electron micrographs of cross-section of PEO coatings (a) PPEO (b) PPEO(M) (c) PPEO(L).

the other hand, large-sized pores are sealed by solidified material, especially in the case of PPEO(M). As for PPEO(L), the surface is dominated by many tiny pores, which are in the range of 1–5 μm. Interestingly, many particles and fibers together with solidified material are piled up in some large-sized pores of PPEO(M) (Fig. 2d), which is in agreement with the original particles morphology. In addition, all coatings are also dominated by many hairline micro-cracks, which may result from thermal stress due to rapid solidification of molten material in the relatively cool electrolyte [12]. As for the PPEO(S), the coating surface is brittle and full of cracks, as can be seen in Fig. 2b.

The backscattered scanning electron micrographs showing the cross-sectional feature of the PEO coated specimens obtained from the different electrolytes are presented in Fig. 3. The PPEO consists of three parts: outer layer, pore band and inner layer. The build-up of the PEO coatings has not been varied by particle addition. Some large-sized pores (3–12 μm) can be observed in the outer layer of PPEO and PPEO(M). In contrast, the size of the defects of PPEO(L) is a little bit smaller (1–4 μm). Many cracks reaching from the pore band towards the outer layer can be observed for the PPEO(M). Interestingly, pore band can hardly be observed between outer layer and inner layer for PPEO(L), but larger magnification reveal that it is still present. The growth rate of coating produced from electrolyte without particle addition is much faster than in the case of Si_3N_4 addition, resulting in PPEO with an average layer thickness of 40 μm compared to PPEO(M) (25 μm) and PPEO(L) (10 μm). Some large-sized pores can be observed at the outer layer for all coatings. Moreover, some particles are found incorporated in the outer layer even reaching inner layer in Fig 3b and c, indicating that they might not react with other material during PEO processing.

3.3. Chemical and phase composition

The composition of near surface of PEO coatings is given in Table 1. The content of O, Mg, P and Na of PEO coatings with particle addition is less but nearly the same compared to PPEO, which is consistent with the additional presence of Si. More particles seem to be incorporated in PPEO(L) (9%) than PPEO(M)(7%). However, it might be caused by the particle size and not by the number of particles incorporated.

To study the distribution of Si_3N_4 particles in the cross section of PEO coatings with particle addition, elemental mapping by EDS was carried out and is shown in Figs. 4 and 5. The elements Si, Mg, O and P were detected in both PEO coatings. Because light elements below oxygen cannot be routinely analyzed by EDS in our system, the distribution of nitrogen is not given. However, the uniform distribution of particles indicated by intensity dots of Si, which can be observed across the whole cross section of the PEO coatings obtained with particle addition. Some dots seem to be larger than the original particle size. Due to some defects (pores), small Si_3N_4 particles might be piled up to a

Table 1
Surface composition of the PEO coatings determined by EDS analysis.

Concentration (at. %)	O	Mg	P	Na	Si
PPEO	65	20	10	5	0
PPEO(M)	63	19	7	4	7
PPEO(L)	60	18	8	5	9

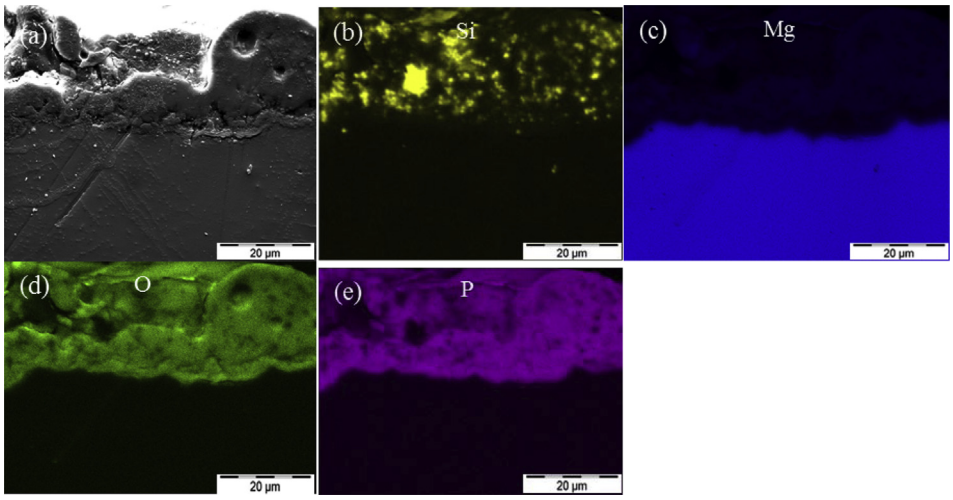

Fig. 4. Elemental mapping of PPEO(M) obtained by EDS (a) SEM image of cross section (b) Si (c) Mg (d) O (e) P.

large volume in specific areas. Phosphorus and oxygen also distribute uniformly in the two PEO coatings. With respect to the magnesium, signal form substrate is stronger than the coating as one would expect.

The PPEO coating is found to be constituted by MgO and $Mg_3(PO_4)_2$ phases, as evidenced from the XRD pattern in Fig. 6. In addition, there are some magnesium peaks, indicating the X-ray could penetrate the layer reaching the magnesium substrate. In PEO coatings achieved from electrolytes with particle addition, many Si_3N_4 peaks and a small peak corresponding to MgO have been found. No crystalline phase containing phosphorus can be detected even though P is seen in EDS analysis, which might be influenced by the addition of particles. As the XRD pattern contains Si_3N_4 peaks and the elemental mapping analysis shows the existence of particles, it confirms that Si_3N_4 particles may have not or not completely reacted to new phases during PEO processing. In other words, the discharge energy cannot melt Si_3N_4 particles, which indicates that the energy of the discharges occurring in these two electrolytes under the applied processing parameters is lower than the melting temperature (1900 °C) of Si_3N_4.

3.4. Corrosion behavior

3.4.1. Potentiodynamic polarization

The corrosion behavior of PEO coatings evaluated by potentiodynamic polarization technique after exposure of 0.5 h in 0.5 wt.% NaCl solution is presented in Fig. 7. The corrosion potential (E_{corr}), corrosion current density (i_{corr}) and the breakdown potential (E_{bd}) derived from potentiodynamic polarization plots are summarized in Table 2.

From Table 2, the free corrosion potentials of PEO coatings are found to be in the active direction to that of the bare alloy, especially for PPEO(M) and PPEO(L). The corrosion potential of AM50 magnesium alloy with a phosphate based PEO coating was found to be slightly active than the magnesium substrate [13]. Interestingly, the corrosion potentials of the PEO coatings with particle addition drift towards more active

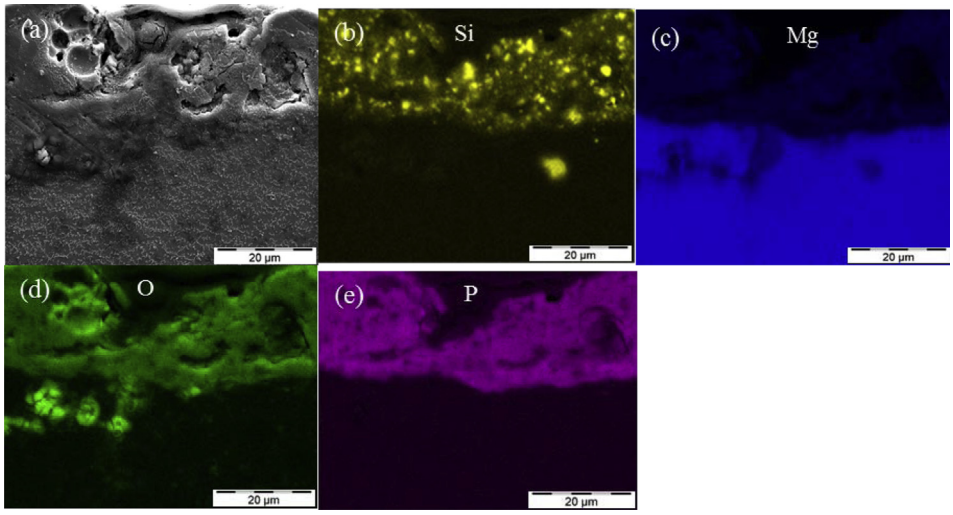

Fig. 5. Elemental mapping of PPEO(L) obtained by EDS (a) SEM image of cross section (b) Si (c) Mg (d) O (e) P.

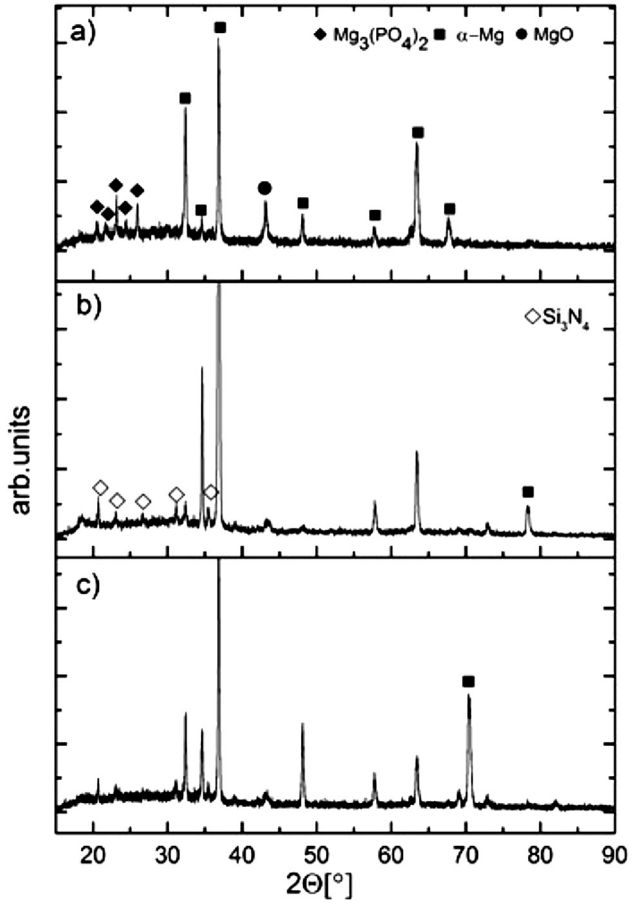

Fig. 6. X-ray diffraction patterns of three PEO coatings (a) PPEO (b) PPEO(M) (c) PPEO(L).

side than PPEO, which might be contributed to the presence of particles containing in the coating. It can also be seen that the i_{corr} values of PPEO(M) and PPEO(L) are in the same order of magnitude in the 0.5 wt. % NaCl solution, whilst the i_{corr} value of PPEO is lower to some extent. The relatively higher corrosion current of PPEO(M) might be caused by the thinner layer and several cracks between the outer layer and the inner

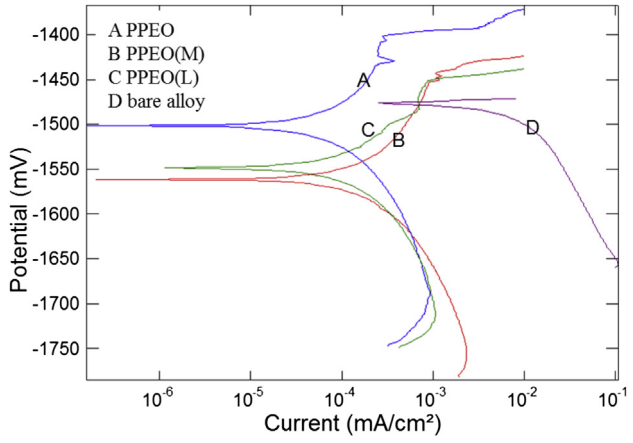

Fig. 7. Potentiodynamic polarization behavior of the specimens PEO coated in electrolytes containing different sized particles (test electrolyte: 0.5 wt.% NaCl).

Table 2
Electrochemical data for PEO coated specimens from potentiodynamic polarization studies.

Coating	E_{corr} (mV)	i_{corr} (mA cm^{-2})	E_{bd} (mV)
PPEO	−1509 ± 9	(9 ± 0.5) × 10^{-5}	−1400 ± 20
PPEO(M)	−1559 ± 2	(1.9 ± 0.2) × 10^{-4}	−1436 ± 16
PPEO(L)	−1575 ± 27	(1.3 ± 0.1) × 10^{-4}	−1445 ± 6
Bare alloy	−1452 ± 10	(3.5 ± 1.1) × 10^{-2}	–

layer. Even though the PPEO(L) is the thinnest layer, its corrosion behavior is not that bad due to fewer defects on the cross section. Generally, the breakdown potential (E_{bd}) of coated alloys in corrosive environments is considered as an indication of the capability of a coating to resist localized corrosion damage [14]. The PPEO seems to be more stable on the basis of higher breakdown potential (−1400 ± 20 mV) in contrast with other two coatings. However, the polarization required to reach breakdown potential from the free corrosion potential is for all the coatings nearly the same.

3.4.2. EIS behavior

The corrosion deterioration of PEO coated specimens in 0.5 wt. % NaCl with prolonged immersion time up to 72 h was examined by EIS measurements. The EIS spectra (Bode plots) of PEO coatings obtained from different electrolytes are presented in Fig. 8.

Based on the impedance plots, taking into account the microstructure of PEO coatings and EIS studies of Liang et al. [15] and Ghasemi et al. [16] on coatings, an appropriate equivalent circuit is given in Fig. 9 and the results are documented in Tables 3–5. The elements in equivalent circuit include R_s (the solution resistance), R_p (resistance of outer porous layer) paralleled with CPE_p (a constant phase element representing the porous outer layer/coating capacitance), R_i (resistance of inner layer) paralleled with constant phase element CPE_i (constant phase element representing the inner layer capacitance).

The Bode plots of PPEO coating after different durations of exposure to the corrosive environment are shown in Fig. 8a and the corresponding electrochemical parameters are presented in Table 3. The resistance of inner layer (R_i) in the EIS test after 0 h of immersion time is 2.35E5 Ω cm^2, with the resistance of the porous layer (R_p) is 63,868 Ω cm^2. The resistance of the R_i and R_p is found to decrease greatly for the tests after 1 h and 3 h immersion, and starts to increase slightly after that until 12 h. The formation of corrosion products and the filling of the pores might be the main reasons for the increase of corrosion resistance. With prolonged exposure the R_p and R_i drop again to lower values. In the case of PEO coatings obtained from electrolyte with particle addition, different trends can be seen from Tables 4 and 5. In the case of PPEO(M), only slight increase of the R_p (from 13,456 Ω cm^2 to 26,097 Ω cm^2) is found after 1 h exposure in 0.5 wt.% NaCl solution. The whole corrosion resistance values decrease rapidly to around 4350 Ω cm^2 after 72 h of exposure. In terms of PPEO(L), no increase of corrosion resistance has been found. However, the R_i after first measurement seems to be

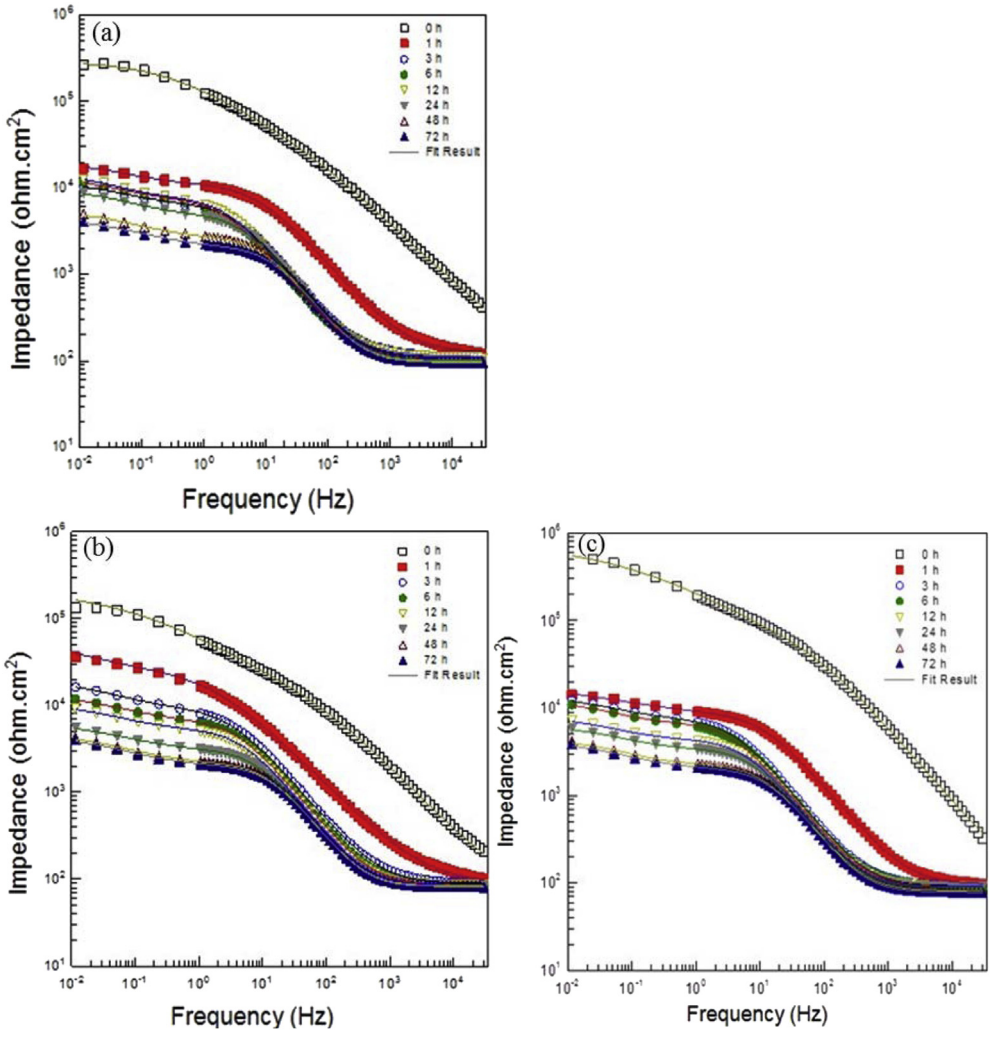

Fig. 8. EIS spectra (Bode plots) of specimens PEO coated obtained from different electrolytes (a) PPEO (b) PPEO(M) (c) PPEO(L) (test electrolyte: 0.5 wt.% NaCl).

larger than other PEO coatings. The R_p and R_i drop continuously to about 2000 Ω cm^2 with the passage of time.

4. Discussions

First of all, it is possible to produce particle-reinforced coatings with addition of relatively large-sized Si_3N_4 particles (0.1–0.8 μm and 1–5 μm). Particles have been found distributed uniformly throughout the cross section of PPEO(M) and PPEO(L). Taking the microstructure and EDS analysis of PEO coatings into consideration, the uniform distribution of particles is caused by two reasons. On the one hand, particles could flow towards the inner coating through discharge channels even reaching the inner layer. On the other hand, Si_3N_4 particles will be pasted on melted material on the surface of the coating and finally the growing coating is embedding them. Pores on the surface of PEO coating have been filled by particles, as can be seen in Fig. 2d anf f. Even though the surface could be optically greatly improved by the particle addition, there is no significant impact on enhancing cross-sectional quality of PEO coatings.

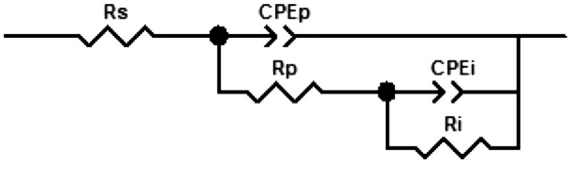

Fig. 9. Equivalent circuits for fitting the impedance data of PEO coatings on AM50 magnesium alloy.

Table 3
Electrochemical fitting data of the PPEO coated specimens from EIS.

Immersion time	R_p, Ω cm^2	(CPE-T)$_p$	(CPE-P)$_p$	R_i, Ω cm^2	(CPE-T)$_i$	(CPE-P)$_i$
0 h	63,868	6.58E-7	0.68	2.35E5	2.15E-6	0.52
1 h	11,224	3.95E-6	0.82	8026	3.27E-4	0.70
3 h	6752	1.21E-5	0.87	4449	7.2E-4	0.75
6 h	7458	1.44E-5	0.87	5353	6.01E-4	0.75
12 h	7620	1.29E-5	0.88	7136	5.46E-4	0.73
24 h	4892	1.15E-5	0.89	4783	6.05E-4	0.72
48 h	2552	1.05E-5	0.91	2965	8.27E-4	0.67
72 h	2035	1.03E-5	0.91	2306	9.1E-4	0.65

Table 4
Electrochemical fitting data of the PPEO(M) coated specimens from EIS.

Immersion time	R_p, Ω cm^2	$(CPE\text{-}T)_p$	$(CPE\text{-}P)_p$	R_i, Ω cm^2	$(CPE\text{-}T)_i$	$(CPE\text{-}P)_i$
0 h	13,456	6.14E-7	0.76	2.02E5	6.37E-6	0.44
1 h	26,097	7.79E-6	0.72	23,526	1.87E-4	0.69
3 h	9547	8.84E-6	0.85	8843	3.45E-4	0.72
6 h	6729	8.74E-6	0.89	6686	4.34E-4	0.66
12 h	5170	9.01E-6	0.91	5415	5.56E-4	0.65
24 h	3016	9.65E-6	0.91	3023	8.19E-4	0.68
48 h	2115	9.59E-6	0.91	2420	9.96E-4	0.68
72 h	1949	9.24E-6	0.92	2401	1.02E-3	0.65

It can also be concluded that mainly an inert incorporation of Si_3N_4 particles (0.1–0.8 μm and 1–5 μm) occurs without reaction with other components of the coating or electrolyte forming new compounds and phases during PEO processing. In other words, the plasma temperature or at least the transferred energy into the coating produced by the discharges during PEO processing from electrolytes with Si_3N_4 particles (0.1–0.8 μm and 1–5 μm) addition is not high enough to reach the melting temperature of Si_3N_4 (1900 °C). The inert particles may be considered as obstacles for coating growth reducing the effective area for formation of conversion products which are finally converted by the discharges into the coating. Furthermore the coating has to grow around the particles thus large-sized particles are bigger obstacles resulting in the observed thinner coatings with increasing particle size. For the electrolyte with the smallest particles (0.02 μm) addition, a normal PEO coating could not be achieved. Coating formation was observed and the breakdown potential was exceeded but a final voltage of 450 V was never reached. The plan view of those specimens revealed severe cracking, with crack opening up to 10 μm and down to the substrate. If this cracking occurs during the processing continuously one can understand that the final voltage cannot be reached because always new substrate is exposed. It might be possible that the nano-sized particles (which are generally known to have lower melting temperatures [17,18]) are being reactive incorporated forming a new and brittle coating phase that cannot withstand the internal stresses generated by the PEO processing. However, this assumption needs further studies to be proven.

In terms of improving corrosion resistance of PEO coating, incorporating Si_3N_4 particles into electrolyte seems to be not effective. Although Si_3N_4 particles are stable and distributed uniformly throughout the cross section, they do not form a dense and thick film. Thus they cannot protect the substrate better than the PPEO coating only. In general, the quality and thickness of the cross section, especially the inner layer, play more important role in the corrosion resistance in contrast with the surface of PEO coating.

Table 5
Electrochemical fitting data of the PPEO(L) coated specimens from EIS.

Immersion time	R_p, Ω cm^2	$(CPE\text{-}T)_p$	$(CPE\text{-}P)_p$	R_i, Ω cm^2	$(CPE\text{-}T)_i$	$(CPE\text{-}P)_i$
0 h	40,641	9.75E-8	0.85	7.21E5	2.04E-6	0.42
1 h	8364	3.12E-6	0.86	8364	2.91E-4	0.56
3 h	7432	8.21E-6	0.89	5899	5.03E-4	0.70
6 h	6757	9.44E-6	0.89	4875	6.56E-4	0.76
12 h	4273	9.36E-6	0.90	3410	8.64E-4	0.72
24 h	3323	9.35E-6	0.91	2895	9.24E-4	0.70
48 h	2193	1.01E-5	0.90	1993	1.16E-3	0.75
72 h	1934	9.30E-6	0.92	2231	1.10E-3	0.65

5. Conclusions

1) No dense PEO coatings can be produced in the electrolyte containing Si_3N_4 particles with average size of 0.02 μm using the same parameters compared to electrolytes with large-sized particles addition.
2) Si_3N_4 particles are filling pores on the surface but do not densify the cross section. The increasing size of the particles has a negative effect on the thickness of PEO coatings.
3) Si_3N_4 particles are mainly inert incorporated into the coating due to their high melting point.
4) The corrosion resistance of PEO coating has not been improved by addition of external Si_3N_4 particles.

Acknowledgments

The author thanks China Scholarship Council for the award of fellowship and funding to Xiaopeng Lu. The technical support of Mr. Volker Heitmann and Mr. Ulrich Burmester during the course of this work is gratefully acknowledged.

References

[1] A.L. Yerokhin, X. Nie, A. Leyland, A. Matthews, S.J. Dowey, Surf. Coat. Technol. 122 (1999) 73.
[2] E. Matykina, R. Arrabal, F. Monfort, P. Skeldon, G.E. Thompson, Appl. Surf. Sci. 255 (2008) 2830.
[3] A. Kuhn, Met. Finish. 101 (2003) 44.
[4] J. Liang, L. Hu, J. Hao, Electrochim. Acta 52 (2007) 4836.
[5] W. Li, L. Zhu, H. Liu, Surf. Coat. Technol. 201 (2006) 2505.
[6] K.M. Lee, K.R. Shin, S. Namgung, B. Yoo, D.H. Shin, Surf. Coat. Technol. 205 (2011) 3779.
[7] K.M. Lee, B.U. Lee, S.I. Yoon, E.S. Lee, B. Yoo, D.H. Shin, Electrochim. Acta 67 (2012) 6.
[8] M. Laleh, A.S. Rouhaghdam, T. Shahrabi, A. Shanghi, J. Alloys Compd. 496 (2010) 548.
[9] R. Arrabal, E. Matykina, P. Skeldon, G.E. Thompson, J. Mater. Sci. 43 (2008) 1532.
[10] M. Aliofkhazraei, A.S. Rouhaghdam, Appl. Surf. Sci. 258 (2012) 2093.
[11] L. Wang, W. Fu, L. Chen, J. Alloys Compd. 509 (2011) 7652.
[12] H. Duan, C. Yan, F. Wang, Electrochim. Acta 52 (2007) 3785.
[13] P.B. Srinivasan, J. Liang, C. Blawert, M. Störmer, W. Dietzel, Appl. Surf. Sci. 256 (2010) 4017.
[14] G.-L. Song, Surf. Coat. Technol. 203 (2009) 3618.
[15] J. Liang, P.B. Srinivasan, C. Blawert, M. Stormer, W. Dietzel, Electrochim. Acta 54 (2009) 3842.
[16] A. Ghasemi, V.S. Raja, C. Blawert, W. Dietzel, K.U. Kainer, Surf. Coat. Technol. 202 (2008) 3513.
[17] A.F. Lopeandía, J. Rodríguez-Viejo, Thermochim. Acta 461 (2007) 82.
[18] W.H. Qi, M.P. Wang, Mater. Chem. Phys. 88 (2004) 280.